metals

MDPI

Supplementary Materials

Designing Quaternary and Quinary Refractory-Based High-Entropy Alloys: Statistical Analysis of their Lattice Distortion, Mechanical, and Thermal Properties

Saro San [1], Sahib Hasan [1,2], Puja Adhikari [1] and Wai-Yim Ching [1,*]

[1] Department of Physics and Astronomy, University of Missouri-Kansas City, Kansas City, MO 64110, USA; saro1990@gmail.com (S.S.); sahmvd@mail.umkc.edu (S.H.); paz67@umkc.edu (P.A.)
[2] Department of Sciences, College of Basic Education, Al Muthanna University, Samawah 66001, Iraq
* Correspondence: chingw@umkc.edu

1. Materials and Methods

Debye temperature (Θ_D) and the average sound velocity (v_m) can be calculated as follows [1–4]:

$$\Theta_D = \frac{h}{k_B}\left[\frac{3n}{4\pi}\left(\frac{N_A.\rho}{M}\right)\right]^{\frac{1}{3}} v_m \quad (S1)$$

$$v_m = \left[\frac{1}{3}\left(\frac{2}{v_s^3} + \frac{1}{v_l^3}\right)\right]^{-\frac{1}{3}} \quad (S2)$$

Here, ρ is the theoretical density of the solid solution model, and h, k_B, and N_A are Planck's constant, Boltzmann constant, and Avogadro's number, respectively. M is the molecular weight and n is the number of atoms in the supercell. v_s and v_l are the transverse (shear) and longitudinal sound velocities, respectively. The compressional (longitudinal) waves and shear waves are estimated by using the values of bulk modulus (K) and shear modulus (G) according to the Voigt–Reuss–Hill approach based on the following formulas [5]:

$$v_s = \sqrt{\frac{G}{\rho}} \quad (S3)$$

$$v_l = \sqrt{\frac{3K + 4G}{3\rho}} \quad (S4)$$

An empirical formula was used for calculating an estimation of melting temperature(T_{melt}) with a standard error of about ±300 K by using the elastic constants[6–8]:

$$T_{melt} = \left[553K + \left(\frac{5.91K}{GPa}\right) C_{11}\right] \mp 300K \quad (S5)$$

Clarke's formula for the minimum thermal conductivity (κ_{min}) is given as follows[9,10]:

$$\kappa_{min} = 0.87 k_B \left(\frac{N_A.n.\rho}{M}\right)^{\frac{2}{3}} \sqrt{\frac{E}{\rho}} \quad (S6)$$

Cahill's formula for the minimum thermal conductivity is given by[11,12]

$$\kappa_{min} = \frac{k_B}{2.48}\left(\frac{n}{V}\right)^{\frac{2}{3}} (v_l + 2v_s) \quad (S7)$$

Slack's formula[13,14] for thermal conductivity (κ) or for lattice thermal conductivity (κ_L) (in case the electronic part of thermal conductivity (κ_e) is negligible) is given by

$$\kappa = A\frac{M_{ave}{\Theta_D}^3\Omega}{\left(\gamma_\alpha^2.n^{\frac{2}{3}}.T\right)} \quad (S8)$$

$$M_{ave} = \frac{M}{n.N_A} \quad (S9)$$

where V is the volume of the supercell, and A is a constant that can be approximated to be 3.1e-6[14] when κ in W.m^{-1}.K^{-1}. Γ_α is the acoustic Grüneisen parameter, Ω is the volume per atom, and T is the temperature in Kelvin units.

The mixed model [15] can give an empirical formula for lattice thermal conductivity(κ_L) as follows:

$$\kappa_L = \frac{(6\pi^2)^{\frac{2}{3}}}{4\pi^2}.\frac{M_{ave}v_s^3}{V^{\frac{2}{3}}\gamma^2 T} \quad (S10)$$

The acoustic Grüneisen constant (γ_α) was calculated by using the following formula [16]:

$$\gamma_\alpha = \frac{3}{2}\left(\frac{3v_l^2 - 4v_s^2}{v_l^2 + 2v_s^2}\right) \quad (S11)$$

The thermal expansion coefficient (α) can be roughly estimated from the following formula using the value of shear modulus [17]:

$$\alpha = \frac{1.6x10^{-3}}{G} \quad (S12)$$

The maximum value of phonon wavelength (λ_{dom}) can be roughly estimated at any temperature by using the following formula [9]:

$$\lambda_{dom} = \frac{12.566v_m}{T}x10^{-12} \quad (S13)$$

2. Supplementary Figures

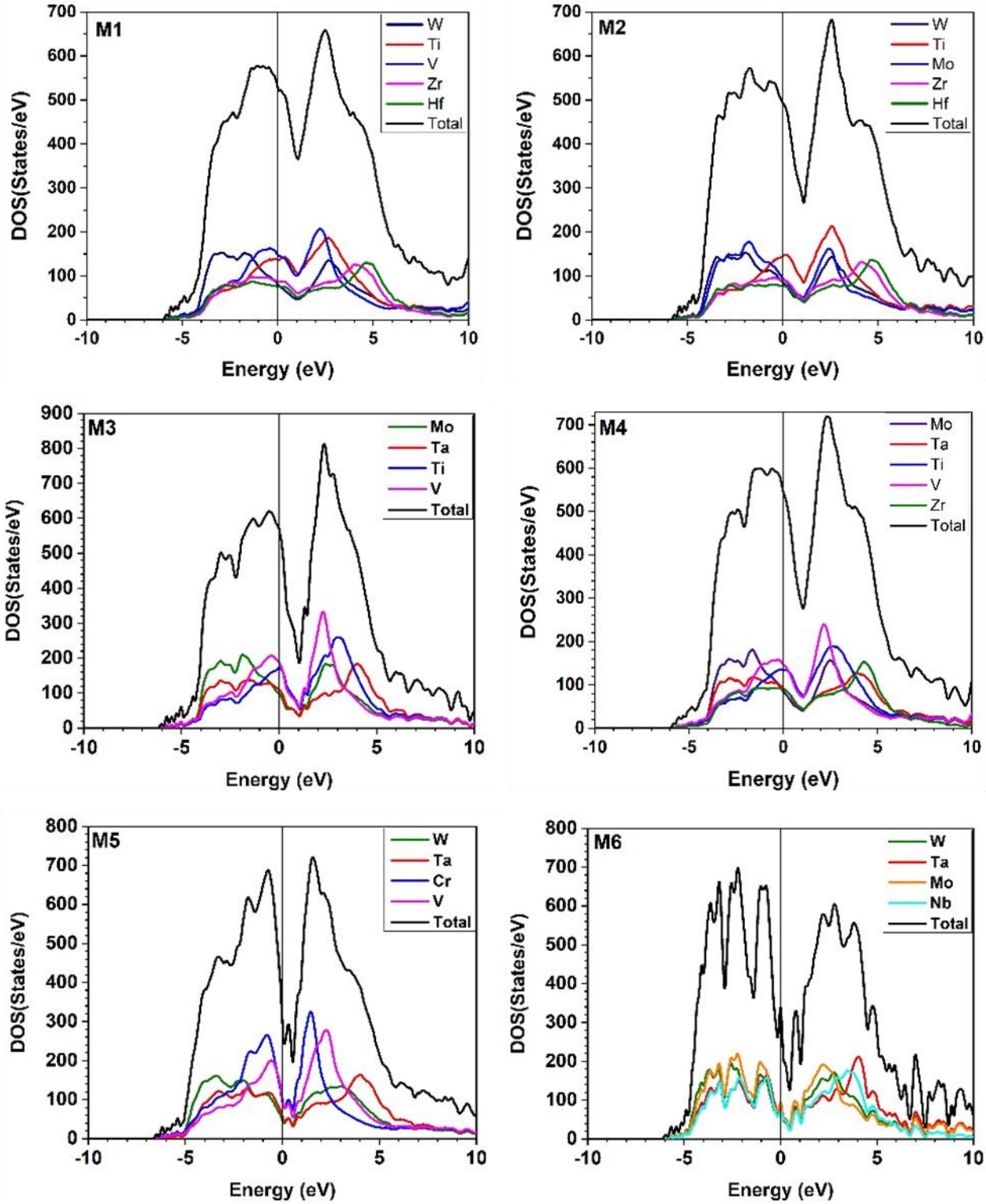
M1
W
Ti
V
Zr
Hf
Total
M2
W
Ti
Mo
Zr
Hf
Total
M3
Mo
Ta
Ti
V
Total
M4
Mo
Ta
Ti
V
Zr
Total
M5
W
Ta
Cr
V
Total
M6
W
Ta
Mo
Nb
Total
DOS(States/eV)
Energy (eV)

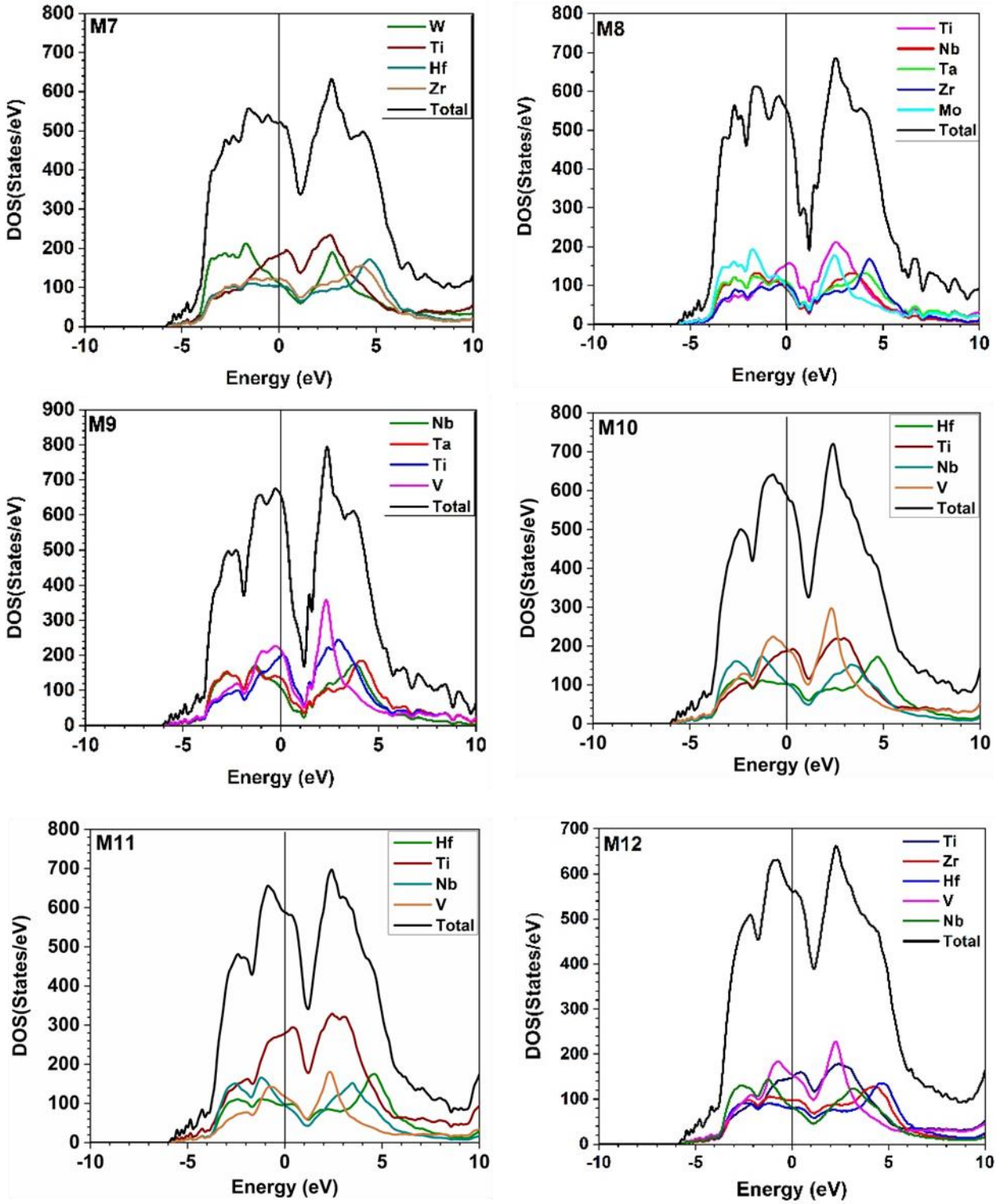

Figure S1. Calculated total density of states (TDOSs) and partial density of states (PDOSs) of the 12 *bcc* HEAs models.

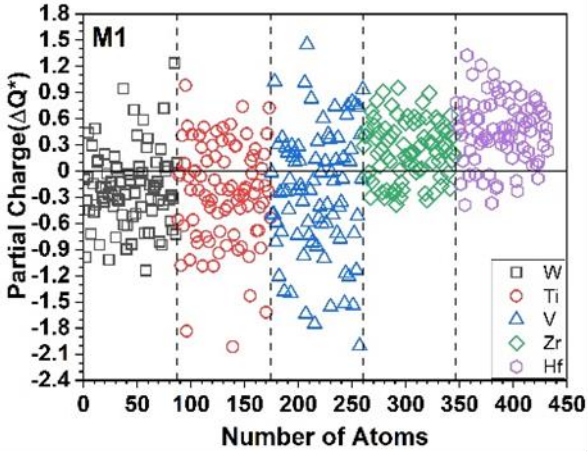
M1
Partial Charge(ΔQ*)
Number of Atoms
W
Ti
V
Zr
Hf

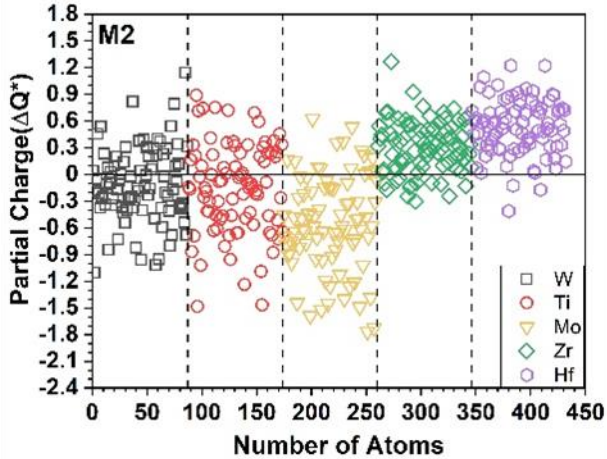
M2
Partial Charge(ΔQ*)
Number of Atoms
W
Ti
Mo
Zr
Hf

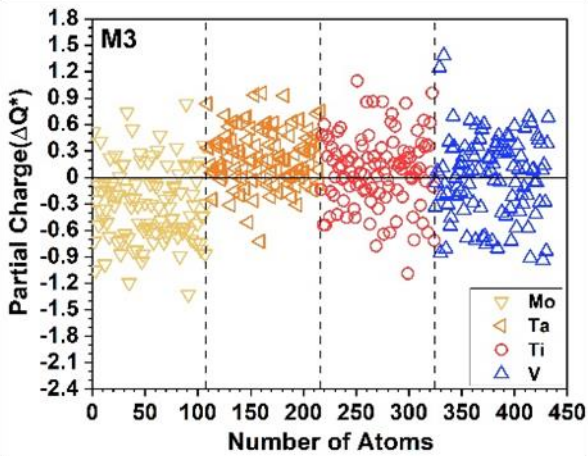
M3
Partial Charge(ΔQ*)
Number of Atoms
Mo
Ta
Ti
V

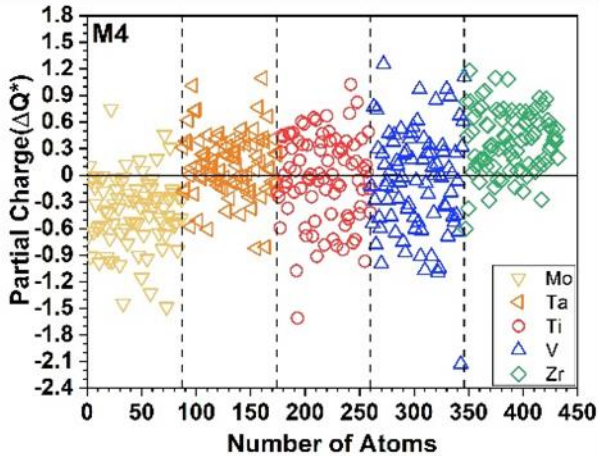
M4
Partial Charge(ΔQ*)
Number of Atoms
Mo
Ta
Ti
V
Zr

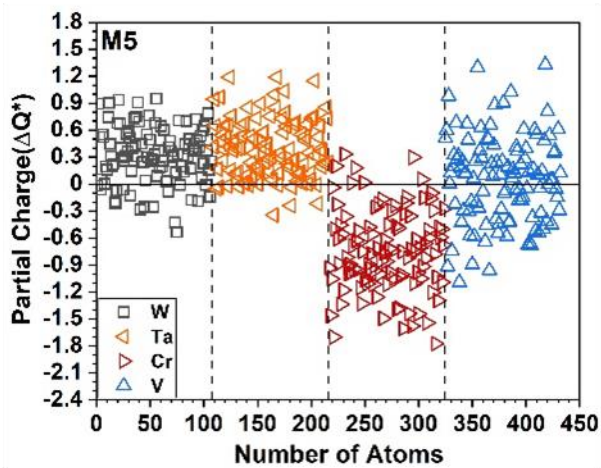
M5
Partial Charge(ΔQ*)
Number of Atoms
W
Ta
Cr
V

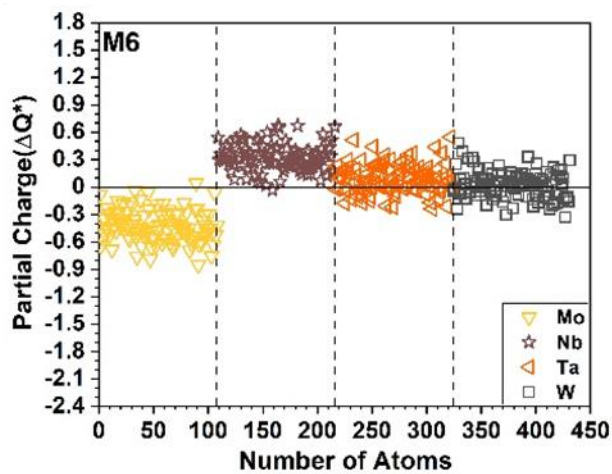
M6
Partial Charge(ΔQ*)
Number of Atoms
Mo
Nb
Ta
W

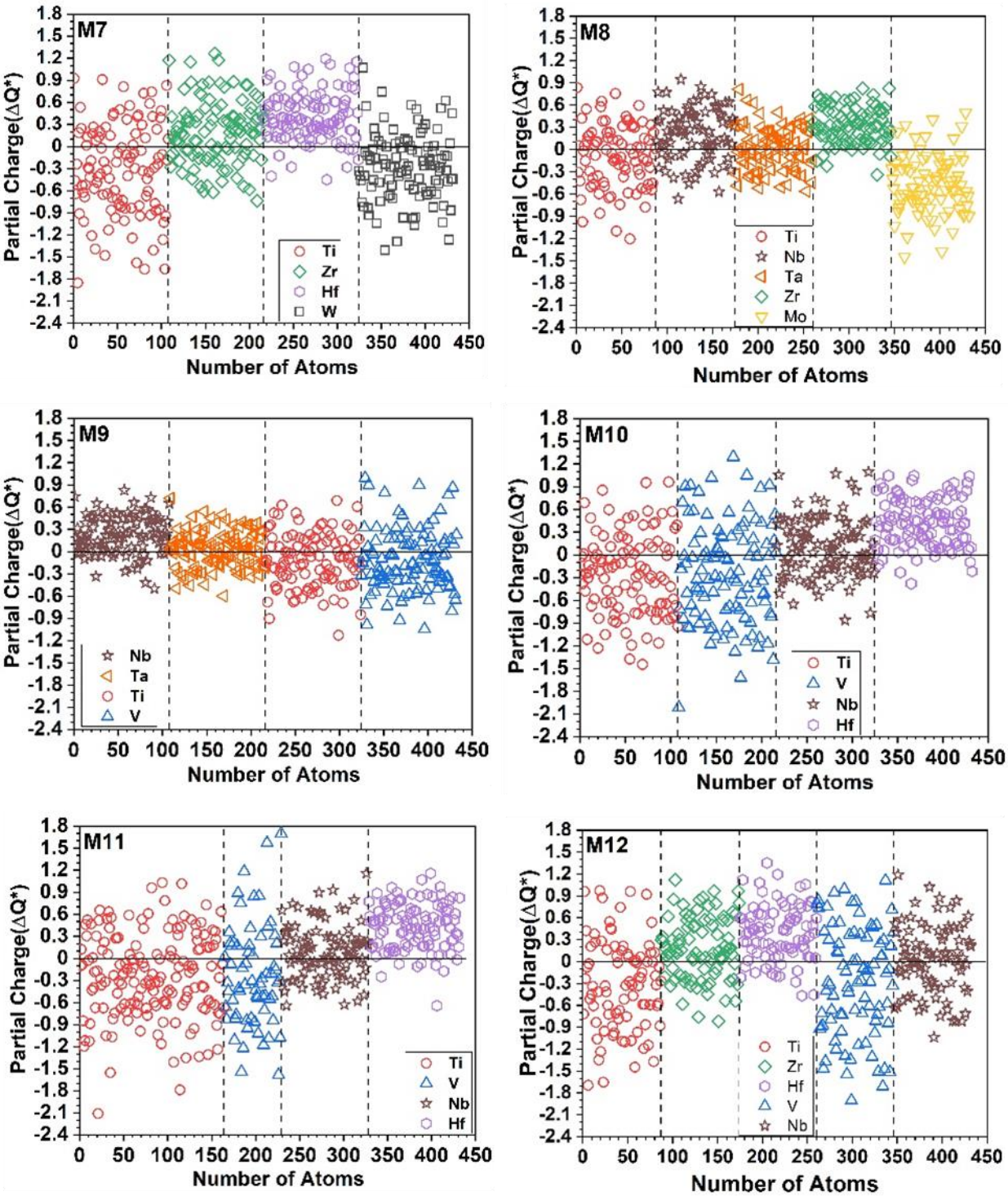

Figure S2. Calculated partial charge (PC) distribution of the 12 *bcc* HEAs models.

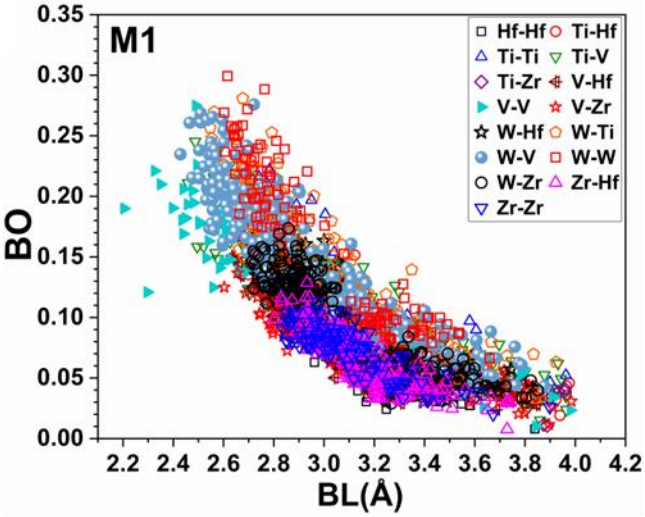
M1
Hf-Hf
Ti-Hf
Ti-Ti
Ti-V
Ti-Zr
V-Hf
V-V
V-Zr
W-Hf
W-Ti
W-V
W-W
W-Zr
Zr-Hf
Zr-Zr
BO
BL(Å)

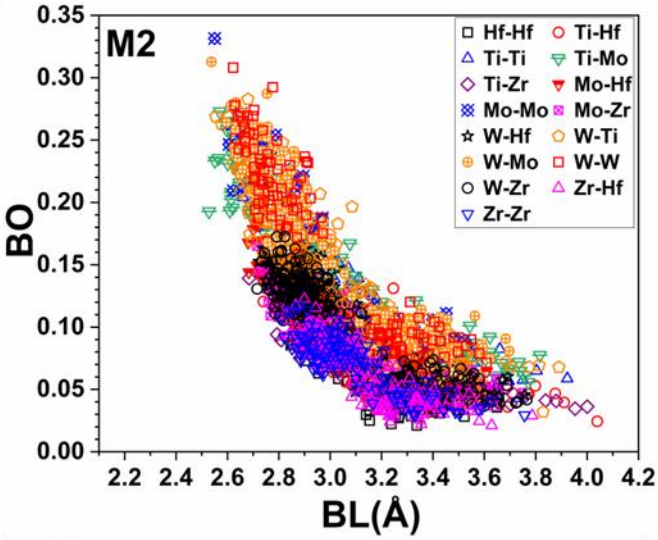
M2
Hf-Hf
Ti-Hf
Ti-Ti
Ti-Mo
Ti-Zr
Mo-Hf
Mo-Mo
Mo-Zr
W-Hf
W-Ti
W-Mo
W-W
W-Zr
Zr-Hf
Zr-Zr
BO
BL(Å)

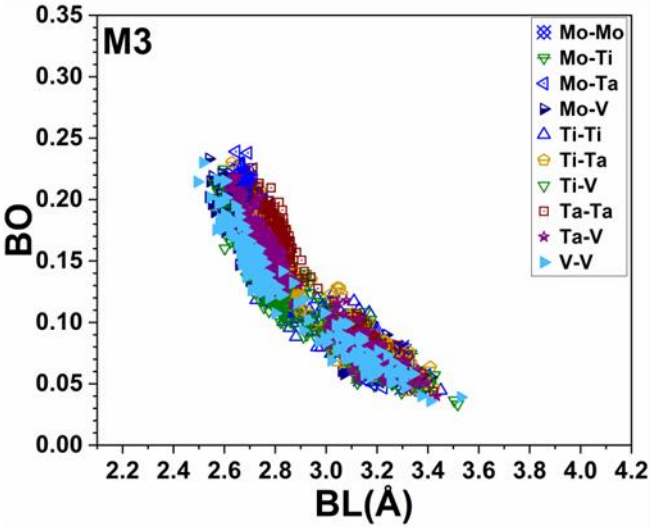
M3
Mo-Mo
Mo-Ti
Mo-Ta
Mo-V
Ti-Ti
Ti-Ta
Ti-V
Ta-Ta
Ta-V
V-V
BO
BL(Å)

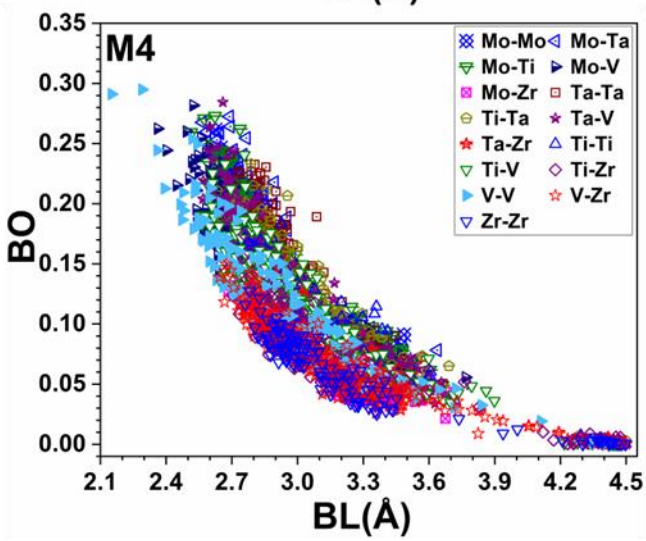
M4
Mo-Mo
Mo-Ta
Mo-Ti
Mo-V
Mo-Zr
Ta-Ta
Ti-Ta
Ta-V
Ta-Zr
Ti-Ti
Ti-V
Ti-Zr
V-V
V-Zr
Zr-Zr
BO
BL(Å)

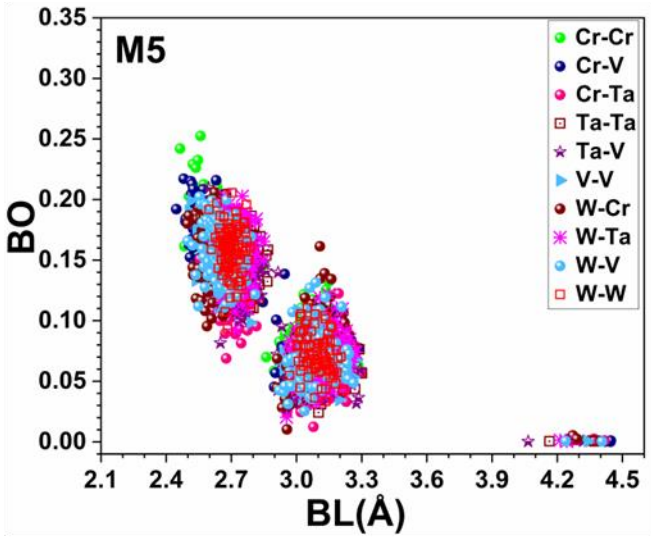
M5
Cr-Cr
Cr-V
Cr-Ta
Ta-Ta
Ta-V
V-V
W-Cr
W-Ta
W-V
W-W
BO
BL(Å)

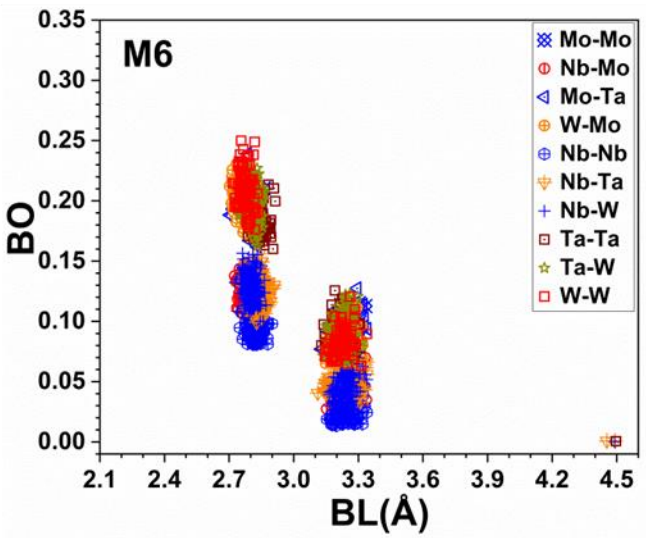
M6
Mo-Mo
Nb-Mo
Mo-Ta
W-Mo
Nb-Nb
Nb-Ta
Nb-W
Ta-Ta
Ta-W
W-W
BO
BL(Å)

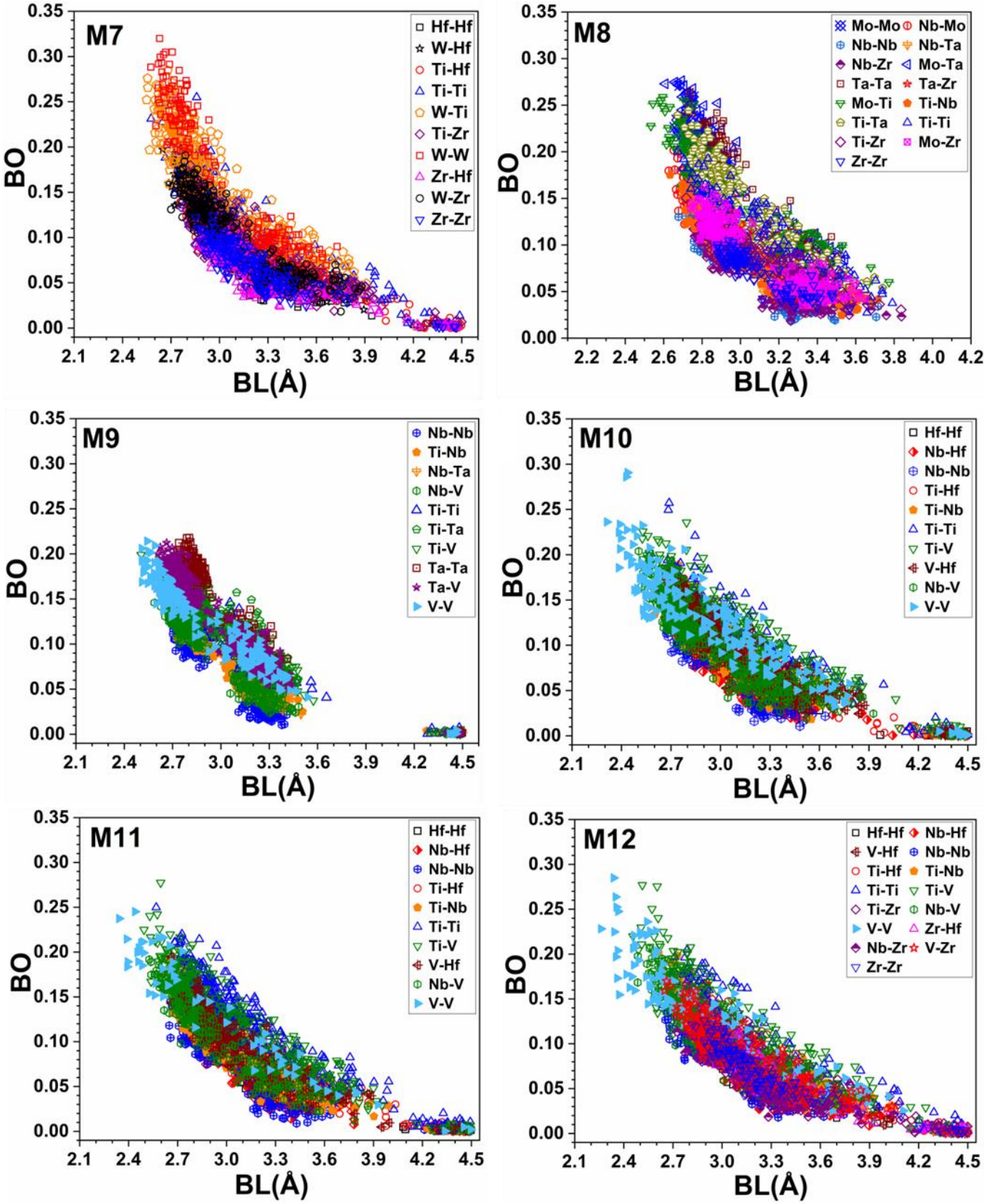

Figure S3. Calculated bond order (BO) versus bond length (BL) of the 12 *bcc* HEAs models.

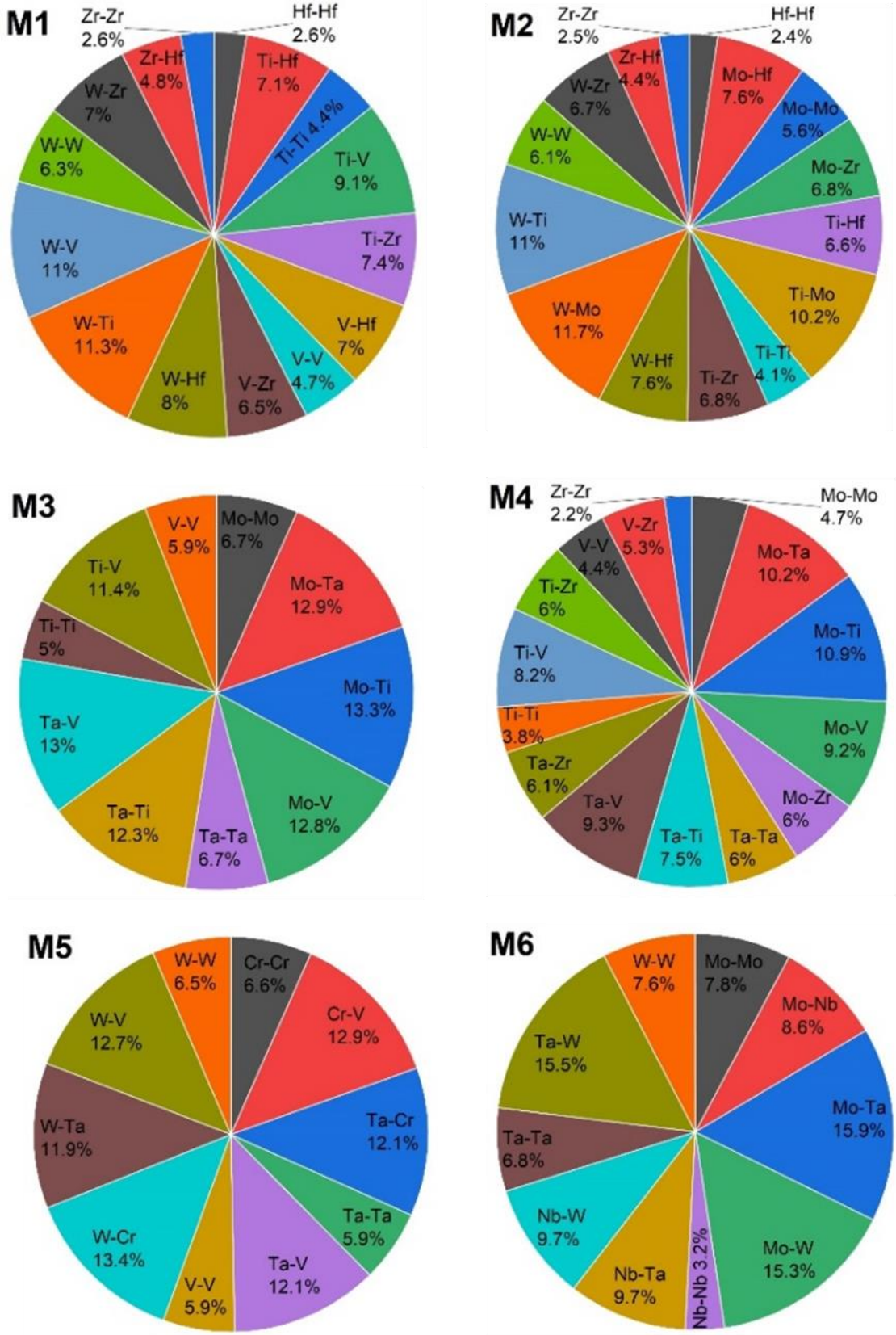
M1
Zr-Zr 2.6%
Hf-Hf 2.6%
Zr-Hf 4.8%
Ti-Hf 7.1%
W-Zr 7%
Ti-Ti 4.4%
W-W 6.3%
Ti-V 9.1%
W-V 11%
Ti-Zr 7.4%
W-Ti 11.3%
V-Hf 7%
V-V 4.7%
W-Hf 8%
V-Zr 6.5%
M2
Zr-Zr 2.5%
Hf-Hf 2.4%
Zr-Hf 4.4%
Mo-Hf 7.6%
W-Zr 6.7%
Mo-Mo 5.6%
W-W 6.1%
Mo-Zr 6.8%
W-Ti 11%
Ti-Hf 6.6%
Ti-Mo 10.2%
W-Mo 11.7%
Ti-Ti 4.1%
W-Hf 7.6%
Ti-Zr 6.8%
M3
V-V 5.9%
Mo-Mo 6.7%
Ti-V 11.4%
Mo-Ta 12.9%
Ti-Ti 5%
Mo-Ti 13.3%
Ta-V 13%
Ta-Ti 12.3%
Mo-V 12.8%
Ta-Ta 6.7%
M4
Zr-Zr 2.2%
Mo-Mo 4.7%
V-Zr 5.3%
V-V 4.4%
Mo-Ta 10.2%
Ti-Zr 6%
Mo-Ti 10.9%
Ti-V 8.2%
Ti-Ti 3.8%
Mo-V 9.2%
Ta-Zr 6.1%
Mo-Zr 6%
Ta-V 9.3%
Ta-Ti 7.5%
Ta-Ta 6%
M5
W-W 6.5%
Cr-Cr 6.6%
W-V 12.7%
Cr-V 12.9%
W-Ta 11.9%
Ta-Cr 12.1%
Ta-Ta 5.9%
W-Cr 13.4%
Ta-V 12.1%
V-V 5.9%
M6
W-W 7.6%
Mo-Mo 7.8%
Mo-Nb 8.6%
Ta-W 15.5%
Mo-Ta 15.9%
Ta-Ta 6.8%
Nb-W 9.7%
Mo-W 15.3%
Nb-Ta 9.7%
Nb-Nb 3.2%

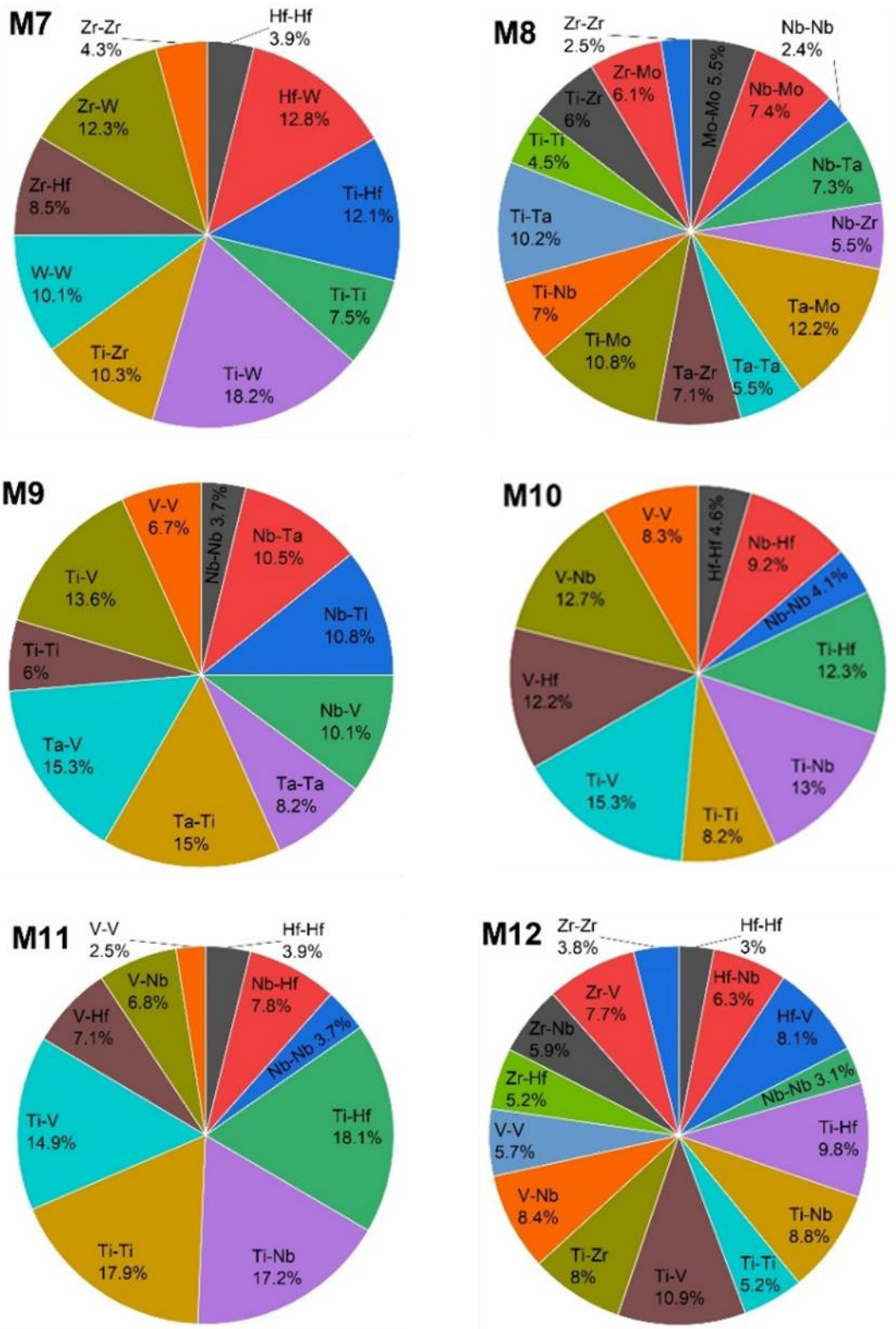

Figure S4. The pie charts show the percentages of different bonding types of the 12 *bcc* HEAs models.

3. Supplementary Discussion

From **Fig.S3**, we notice the following:

1. Hf–Hf bonds distribute over a 2.8−3.9 Å BL with a small BO in M1, M2, and M12, while for M10 and M11, they distribute over relatively shorter BLs, ranging from 2.85 to 3.65 Å for M10 and 2.8 to 3.5 Å for M1.

2. Ti–Ti bonds distribute over a 2.6–4.5 Å BL with BO distributed 0.0–0.20e$^-$ in M1, M2, M3, M4, and M12, while for M10 and M11, they distribute along longer BLs, ranging from 2.5 to 4.55 Å with BO distributed from 0.0 to 0.25 e$^-$.

3. Ti–Zr bonds distribute over a 2.6–3.9 Å BL with BO distributed 0.025–0.17 in M1, M2, M4, and M12, while they distribute 2.6–3.75 Å with BO distributed 0.025–0.15 e$^-$ in M8.

4. V–V bonds distribute over 2.4–4.5 Å in M9, M10, and M11, while they distribute along shorter BLs in M1, M3, and M12.

5. W–Mo bonds distribute over 2.5–3.7 Å with BO distributed 0.05–0.31 e$^-$ in M2, while they distribute along a shorter BL (2.7–3.3 Å) with BO distributed 0.05–0.24 e$^-$ in M6.

6. Ti–Mo bonds distribute over 2.5–3.8 Å with BO distributed from 0.04–0.27 in M2 and M8, while they distribute along a shorter BL (2.5–3.5 Å) with BO distributed from 0.05–0.28 in M3 and M4.

7. Mo–Ta bonds distribute over 2.6–3.3 Å in M6, while they distribute along longer BL in M3, M4, and M8.

8. Ti–Ta bonds distribute over 2.5–4.5 Å with BO distributed 0.0–0.2 in M9, while they distribute along shorter BLs and higher BOs in M3, M4, and M8.

9. Ta–Ta bonds distribute along shorter BLs in M5 and M6 in comparison to M3 and M4

10. V–Hf bonds distribute along wide BLs (2.5–4.5 Å) in M10, M11, and M12.

11. W–W bonds distribute along shorter BLs (2.7–3.3 Å) in M5 and M6 in comparison to M1, M2, and M7.

12. Mo–Mo bonds distribute along shorter BLs (2.6–3.3 Å) in M3 and M6 in comparison to M2, M4, and M8.

13. Ta–Ta bonds distribute along longer BLs (2.6–4.5 Å) in M9 in comparison to M8(2.6–3.6 Å).

14. Ta–V bonds distribute along much wider BLs (2.6–4.5 Å) in M9 in comparison to M3, M4, and M5.

15. Nb–Nb bonds distribute along shorter BLs in M6 in comparison to M8, M9, M10, and M12.

16. Nb–Mo bonds distribute along shorter BLs (2.7–3.3 Å) in M6 in comparison to M8(2.6–3.6 Å).

17. Nb–Ta bonds distribute along much longer BLs (2.7–4.5 Å) in M9 in comparison to M6(2.7–3.3 Å) and M8(2.7–3.7 Å).

18. W–V bonds distribute along shorter BLs (2.5–3.3 Å) in M5 in comparison to M1(2.5–3.9 Å).

19. Ti–Hf bonds distribute along wide BLs (2.6–4.5 Å) in M1, M2, M7, M10, M11, and M12.

20. Nb–V bonds distribute along wide BLs (2.5–4.5 Å) in M9, M10, and M12. **21.** Nb–Hf bonds distribute along wide BLs (2.7–4.5 Å) in M10, M11, and M12.

References

1. Jiang, S.; Shao, L.; Fan, T.W.; Duan, J.M.; Chen, X.T.; Tang, B.Y. Elastic and thermodynamic properties of high entropy carbide (HfTaZrTi)C and (HfTaZrNb)C from ab initio investigation. *Ceram. Int.* **2020**, *46*, 15104–15112.
2. Boudiaf, K.; Bouhemadou, A.; Boudrifa, O.; Haddadi, K.; Saoud, F.S.; Khenata, R.; Al-Douri, Y.; Bin-Omran, S.; Ghebouli, M.A. Structural, Elastic, Electronic and Optical Properties of LaOAgS-Type Silver Fluoride Chalcogenides: First-Principles Study. *J. Electron. Mater.* **2017**, *46*, 4539–4556.
3. Guo, F.; Zhou, X.; Li, G.; Huang, X.; Xue, L.; Liu, D.; Jiang, D. Structural, mechanical, electronic and thermodynamic properties of cubic TiC compounds under different pressures: A first-principles study. *Solid State Commun.* **2020**, *311*, 113856.
4. Anderson, O.L. A simplified method for calculating the Debye temperature from elastic constants. *J. Phys. Chem. Solids* **1963**, *24*, 909–917.
5. Wachter, P.; Filzmoser, M.; Rebizant, J. Electronic and elastic properties of the light actinide tellurides. *Phys. B Condens. Matter* **2001**, *293*, 199–223.
6. Fine, M.E.; Brown, L.D.; Marcus, H.L. Elastic constants versus melting temperature in metals. *Scr. Metall.* **1984**, *18*, 951–956.
7. Benkaddour, K.; Chahed, A.; Amar, A.; Rozale, H.; Lakdja, A.; Benhelal, O.; Sayede, A. First-principles study of structural, elastic, thermodynamic, electronic and magnetic properties for the quaternary Heusler alloys CoRuFeZ (Z = Si, Ge, Sn). *J. Alloys Compd.* **2016**, *687*, 211–220.

8. Liu, S.Y.; Zhang, S.; Liu, S.; Li, D.J.; Li, Y.; Wang, S. Phase stability, mechanical properties and melting points of high-entropy quaternary metal carbides from first-principles. *J. Eur. Ceram. Soc.* **2021**, *41*, 267–6274. doi:10.1016/j.jeurceramsoc.2021.05.022.
9. Clarke, D.R. Materials selections guidelines for low thermal conductivity thermal barrier coatings. *Surf. Coatings Technol.* **2003**, *163–164*, 67–74.
10. Clarke, D.R.; Levi, C.G. Materials design for the next generation thermal barrier coatings. *Annu. Rev. Mater. Res.* **2003**, *33*, 383–417.
11. Cahill, D.G.; Watson, S.K.; Pohl, R.O. Lower limit to the thermal conductivity of disordered crystals. *Phys. Rev. B* **1992**, *46*, 6131–6140.
12. Cahill, D.G.; Ford, W.K.; Goodson, K.E.; Mahan, G.D.; Majumdar, A.; Maris, H.J.; Merlin, R.; Phillpot, S.R. Nanoscale thermal transport. *J. Appl. Phys.* **2003**, *93*, 793–818.
13. Morelli, D.T.; Slack, G.A. High lattice thermal conductivity solids. *High Therm. Conduct. Mater.* **2006**, 37–68. doi:10.1007/0-387-25100-6_2.
14. Morelli, D.T.; Heremans, J.P. Thermal conductivity of germanium, silicon, and carbon nitrides. *Appl. Phys. Lett.* **2002**, *81*, 5126–5128.
15. Toberer, E.S.; Zevalkink, A.; Snyder, G.J. Phonon engineering through crystal chemistry. *J. Mater. Chem.* **2011**, *21*, 15843–15852.
16. Arab, F.; Sahraoui, F.A.; Haddadi, K.; Bouhemadou, A.; Louail, L. Phase stability, mechanical and thermodynamic properties of orthorhombic and trigonal MgSiN 2: An ab initio study. *Phase Transitions* **2016**, *89*, 480–513.
17. Naher, M.I.; Afzal, M.A.; Naqib, S.H. A comprehensive DFT based insights into the physical properties of tetragonal superconducting Mo5PB2. *Results Phys.* **2021**, *28*, 104612.